

# Mechanics-Based Determination of the Center Roller Displacement in Three-Roll Bending for Smoothly Curved Rectangular Plates

**Jong Gye Shin\*, Jang Hyun Lee**

*Department of Naval Architecture and Ocean Engineering, Seoul National University, Shillim-dong, Kwanak-ku, Seoul 151-742, Korea*

**You Il Kim**

*Division of Research and Development, Daewoo Shipbuilding Co., Koje 656-780, Korea*

**Hyunjune Yim**

*Department of Mechanical Engineering, Hong-Ik University, Sangsoo-dong, Mapo-ku, Seoul 121-791, Korea*

The objective of this paper is to develop a logical procedure to determine the center roller displacement, in the three-roll bending process, which is required in the fabrication of curved rectangular plates with a desired curvature. To this end, the mechanics of the process was analyzed by both analytical and finite element approaches. Comparisons of the results reveal that a simple analytical procedure, based on the beam theory, yields a reasonably accurate relationship between the center roller displacement and residual curvature. With further development and refinement, the procedure proposed in this work has great promise for practical application, particularly for the automation of the process.

**Key Words :** Three-Roll Bending, Finite Element Analysis, Spring-Back

## Nomenclature

$b$  : Width of workpiece  
 $E$  : Young's modulus  
 $E_t$  : Tangent modulus  
 $I$  : Second moment of area  
 $M$  : Bending moment  
 $M_{max}$  : Maximum bending moment  
 $M_Y$  : Bending moment at initial yield  
 $s$  : Arc length of workpiece  
 $s_b$  : Spacing between two consecutive bends in sequential bending  
 $s_T$  : Distance between side rolls (Die width)  
 $t$  : Thickness of workpiece  
 $X, Y$  : Cartesian coordinates  
 $Y_c$  : Displacement of the center roller  
 $\epsilon_{max}$  : Maximum normal strain

$\epsilon_x^{total}$  : Total bending strain  
 $\epsilon_x^e$  : Elastic component of bending strain  
 $\epsilon_x^p$  : Plastic component of bending strain  
 $\eta$  : Normal distance from neutral surface  
 $\theta$  : Angle of deflection of neutral surface  
 $\kappa$  : Curvature  
 $\kappa_L$  : Curvature under loading  
 $\kappa_U$  : Residual curvature after unloading  
 $\kappa_Y$  : Curvature at initial yield  
 $\sigma_Y$  : Yield stress

## 1. Introduction

Roll bending is a very important process in the fabrication of curved plates which are used in ship hulls and large steel structures. However, as emphasized in our previous study (Shin et al., 2001), the parameters of this process are all determined by technicians, simply based upon their personal field experiences. Logical procedures for determining such parameters are required for accurate fabrication as well as for the automation of

\* Corresponding Author,  
**E-mail :** jgshin@snu.ac.kr  
**TEL :** +82-2-710-7129; **FAX :** +82-2-884-3803  
 Department of Naval Architecture and Ocean Engineering, Seoul National University, Shillim-dong, Kwanak-ku, Seoul 151-742, Korea. (Manuscript Received April 10, 2001; Revised September 24, 2001)

the process, which is the ultimate goal of our research. In addition, the use of such procedures may yield “well”-curved plates so that minimal effort will be required in the subsequent line heating process.

While our initial-stage work was concerned with the rolling region on a plate, i. e. where to roll, for a desired shape (Shin et al., 2001), the objective of this paper is to develop a procedure for determining the amount or extent of roll bending, given a desired curvature. To this end, a thorough understanding and realistic modeling of the mechanics involved are necessary.

Several related studies have been published previously. A model for bending steel beams with a rectangular cross section was proposed by Hansen and Jannerup (1979), where the computed residual curvature was shown to agree with experimental results. Oh and Gobayashi (1980) studied the problem of bending a sheet metal by the finite element method (FEM) in conjunction with the large-strain formulation. Their model, however, is unrealistic because the entire sheet is modeled so as to be bent simultaneously.

A realistic and sophisticated model was developed by Yang and Shima (1988) for the continuous bending of a beam. Their model accounts for many details of the process such as the shift of contact points between the beam and rollers and, as a result, the equations in the model are rather complex, but the results were in good agreement with experimental values. A simple model for the sequential bending of a beam on a pressbrake was developed by Hardt et al. (1992). The process is modeled as a series of overlapping three-point bending procedures, and the computed results were also in good agreement with experimental values.

All the previous studies mentioned above deal primarily with the prediction of residual curvature given the amount of bending – often called a *forward mechanics problem*. In practice, particularly for automated roll bending, it would be of more direct interest to determine the amount of bending required for a desired curvature – often called an *inverse mechanics problem*. In the present work, the procedure developed by Hardt

et al. (1992) is modified and extended to solve both forward and inverse problems. In contrast to the one-dimensional beam theory adopted in all analytical models, two-dimensional finite element analyses (FEA) were also conducted in this paper with plane strain elements. The results of these two approaches are compared, and their limitations are discussed.

## 2. Roll Bending Process

The roll bending process is usually performed by a three-roll bending machine (often called the pyramid type, because of the peculiar arrangement of the three rollers), schematically shown in Fig. 1. The entire process of roll bending may be divided into three steps: namely, (1) positioning of a blank plate, (2) lowering of the center roller, and (3) feeding of the plate. In the first step, a flat blank plate is fed into the machine by two rotating side rollers until the plate is properly positioned (Fig. 1(a)). In the second step, the center roller is displaced downward, bending the plate (Fig. 1(b)). In the final step, two side rollers rotate again, so that the plate is bent continuously. A steady state is reached in the third step when the point which was initially in contact with the center roller (that is, point B in Fig. 1(a)) passes through the left-hand roller, with the result that all points between the side rollers undergo the same stress and strain history.

A complete analysis of the entire process described above is a very complicated task due to several reasons. First of all, elasto-plastic analyses are required because neither the elastic nor the plastic strain is negligible compared with the other. Secondly, the deformed shape of a plate in the process is not symmetric with respect to its contact point with the center roller (Yang and Shima, 1988). Finally, the contact between the plate and rollers does not occur at a single point and, furthermore, the contacting regions shift constantly until the steady state in the third step is reached. The second and final effects above are important particularly where large deformations are involved: for example, when bending thin plates.

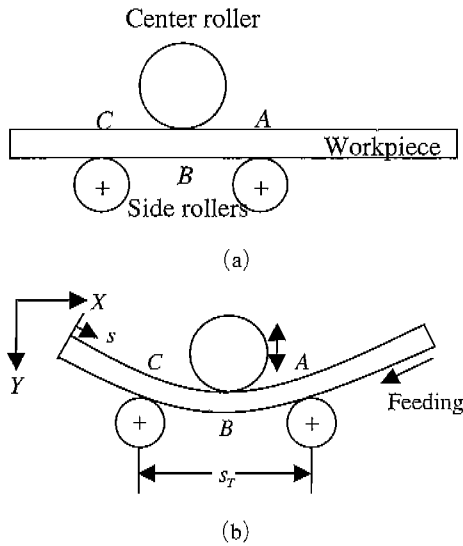


Fig. 1 Schematic diagrams of roll bending process

Considering all these effects in an analytical model does not seem feasible. Therefore, in this paper, an analytical approach based on a simplified model is proposed, and then a more realistic numerical analysis using the FEM is conducted to investigate the validity of the analytical approach.

### 3. Analytical Approach

The analytical approach proposed in this study is a modification and extension of the previous model (Hardt et al., 1992) devised for the sequential bending of beams on a pressbrake. The application of this model to the continuous bending of a plate may be justified for the following reasons. That is, sequential bending approaches continuous bending as the spacing between two consecutive bends is reduced to zero, and a plate may often be modeled as a beam which represents a strip of a unit width taken from the plate (Timoshenko and Woinowsky-Krieger, 1959). This model, however, does not take into account all the complicating effects of continuous bending as described in the previous section. Because the model was described in detail in the literature, only some key equations are repeated and the extended procedure is outlined here.

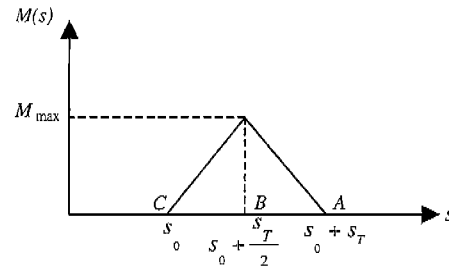


Fig. 2 Distribution of bending moment in a beam under three-point bending

#### 3.1 Equations of mechanics involved

The process in the configuration shown in Fig. 1 may be modeled as a series of three-point bending operations. Equations associated with a single bending are provided in this subsection. A beam undergoing small deformation in three-point bending may be assumed to be subjected to a bending moment distribution,  $M(s)$ , which is a function of the arc length  $s$ , as shown in Fig. 2. That is,

$$M(s) = \begin{cases} \left[ \frac{M_{\max}}{s_T} \right] (s - s_0), & s_0 \leq s \leq s_0 + \frac{s_T}{2} \\ M_{\max} \left[ 2 - \frac{2}{s_T} (s - s_0) \right], & s_0 + \frac{s_T}{2} \leq s \leq s_0 + s_T \end{cases} \quad (1)$$

where  $s_0$ ,  $s_0 + s_T/2$ , and  $s_0 + s_T$  denote the contact points with the left-hand, center, and right-hand rollers, respectively. Note that each roller is assumed here to contact the plate at a point.

By imposing the moment equilibrium requirement over a cross section at  $s$ , it can be shown that  $M(s)$  is related to the corresponding curvature,  $\kappa(s)$ , by

$$M(s) = 2b \int_0^{t/2} \sigma \eta d\eta = \frac{2b}{\kappa^2(s)} \int_0^{(t/2)\kappa(s)} \sigma(\epsilon) \epsilon d\epsilon \quad (2)$$

where, in writing the last equation, a kinematic relationship,  $\epsilon = \kappa\eta$ , has been used; and, the upper integration limit has been replaced by the maximum strain,  $\epsilon_{\max} = (t/2)\kappa(s)$ . Due to the existence of  $\kappa(s)$  in the integration limit, Eq. (2) represents an implicit relationship between  $M(s)$  and  $\kappa(s)$ . Note that Eq. (2) holds for any elasto-plastic constitutive law,  $\sigma(\epsilon)$ . In particular, within elastic limits, Eq. (2) leads to an explicit relationship,  $M(s) = EI\kappa(s)$ , where  $I = bt^3/12$ .

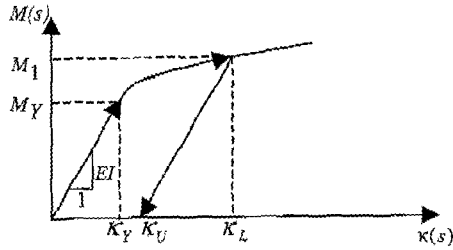


Fig. 3 Relationship between bending moment and curvature

Figure 3 shows a typical relationship between  $M(s)$  and  $\kappa(s)$  at the same section when linearly-elastic strain-hardening behavior is assumed. During a single bending, the maximum curvature will occur at point  $B$  in Fig. 1, i. e. at  $s=s_0+s_T/2$ , where  $M_{max}$  occurs as shown in Fig. 2. The maximum curvature,  $\kappa_{max}$ , is, of course, related to  $M_{max}$  by Eq. (2) when  $M(s)$  and  $\kappa(s)$  in Eq. (2) are replaced by  $M_{max}$  and  $\kappa_{max}$ , respectively. In addition, a case of loading up to an arbitrary moment  $M_1 (> M_Y)$  and subsequent unloading is indicated in Fig. 3 by curves with arrowheads, and the corresponding loaded curvature  $\kappa_L$  and the unloaded (residual) curvature  $\kappa_U$  after spring-back are also shown. The spring-back curvature is given by

$$\kappa_L - \kappa_U = \frac{M_1}{EI} \quad (3)$$

Finally, geometrical equations for the deformed configuration as shown in Fig. 1(b) are necessary. The angle of deflection,  $\theta(s)$ , measured clockwise, and the coordinates,  $(X(s), Y(s))$ , of the neutral surface of the beam may be expressed, in terms of the curvature distribution  $\kappa(s)$ , as

$$\begin{aligned} \theta(s) &= \theta_0 + \int_{s_0}^s \kappa(s) ds \\ X(s) &= X_0 + \int_{s_0}^s \cos \left( \theta_0 + \int_{s_0}^s \kappa(s) ds \right) ds \\ Y(s) &= Y_0 + \int_{s_0}^s \sin \left( \theta_0 + \int_{s_0}^s \kappa(s) ds \right) ds \end{aligned} \quad (4)$$

where the subscripts "0" denote values at  $s=s_0$ .

### 3.2 Computational procedure

Figure 4 shows a flow chart for the computational procedure of the analytical approach.

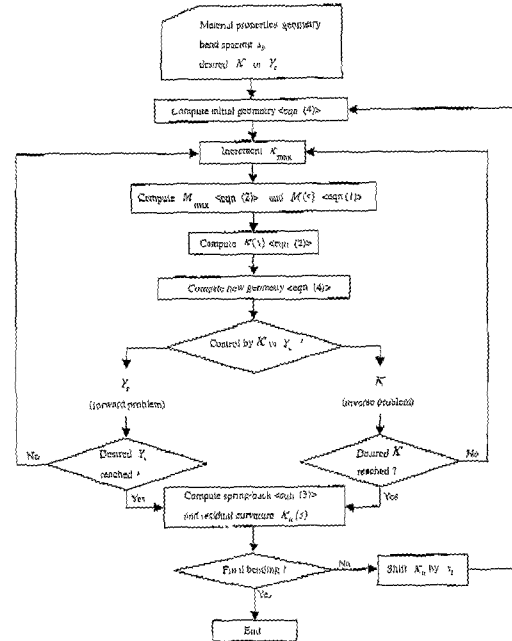


Fig. 4 Flow chart for analytical approach

A nearly identical procedure may be used for the forward problem, i.e. to determine the residual curvature,  $\kappa_U$ , given a constant displacement of the center roller,  $Y_c$ , and for the inverse problem, i.e. to find the value of  $Y_c$  required for a given  $\kappa_U$ . The only difference between these two types of problems lies in the selection between  $Y_c$  or  $\kappa$  as the desired input value, and in the corresponding selection of the left- or right-hand branch in the middle of the flow chart. Therefore, the reader is referred to Hardt et al. (1992), which is concerned with the forward problem, for a detailed explanation of each step in the procedure. The equation number required for each step is indicated in Fig. 4.

Whether a forward or inverse problem is solved, the procedure consists of two nested loops (see Fig. 4). The outer loop is repeated once for each bending until the entire bending sequence is completed. In the inner loop, the deformed shape in a single bending is found by assuming and incrementing the value of  $\kappa_{max}$  until the desired value of  $Y_c$  or  $\kappa$  is reached (Hardt et al., 1992). The residual curvature distribution is then computed by deducting the spring-back curvature

**Table 1** Values of input parameters used

Young's modulus, $E$	200 GPa
Yield stress, $\sigma_Y$	200 MPa
Tangent modulus, $E_t$	50.0 MPa
Plate length, $L$	1.00 m
Plate thickness, $t$	20.0 mm
Distance between side rollers, $s_T$	0.40 m
Rolling range of center roller	$(1/4)L \sim (3/4)L$

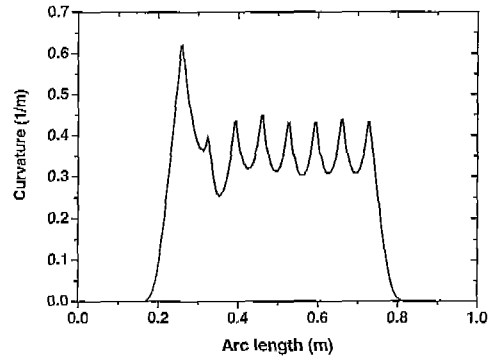
and the analysis proceeds to the next bending, with the curvature distribution shifted by one bend spacing,  $s_b$ .

**3.3 Numerical results**

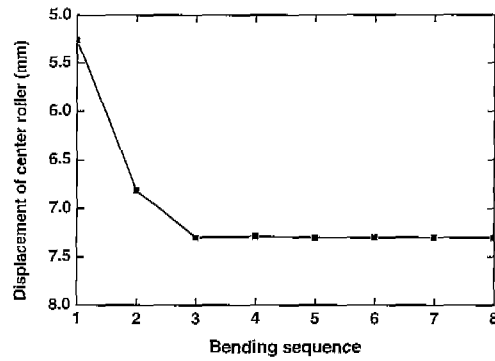
Several numerical results obtained by the analytical approach are illustrated in this subsection. The values of input parameters used are listed in Table 1. The width of the beam in the model is assumed to be unity, as mentioned above.

Figure 5 shows the residual curvature after eight equally-spaced sequential bending operations, computed with the downward center roller displacement,  $Y_c=7.50$  mm (the forward problem). In this analysis, only eight times of sequential bending are assumed because computation required according to the procedure shown in Fig. 4 consumes quite a long time, and because the results may directly compared with those available in the literature as below. It should be emphasized here that in Fig. 5 and all the following figures, only the resulting curvature is shown because the deformed shape, drawn to scale, will not be distinguishable from the original shape due the smallness of the deformation considered here.

It is easily seen from Fig. 5 that the greatest residual curvature is produced by the first bending, the least curvature by the second bending, followed by similar intermediate curvatures afterwards - a steady state. This trend coincides with the previous work (Hardt et al., 1992), where the least curvature in the second bending (called an "undershoot") was attributed to the excessive curvature produced by the previ-



**Fig. 5** Residual curvature distribution after sequential bending



**Fig. 6** Displacements of center roller to obtain constant curvature

ous (first) bending. Note that the small fluctuations in Fig. 5 are due to discrete sequential bending, thus they will be reduced as the bend spacing,  $s_b$ , becomes smaller.

A numerical result for the inverse problem is given in Fig. 6. This figure shows the downward displacements of the center roller in eight sequential bending operations, which are required for a constant residual curvature (see Fig. 7). Conversely, Fig. 7 has been obtained by solving the forward problem using the data in Fig. 6 as the input. It is noteworthy in Fig. 6 that  $Y_c$  in the first two bending operations must be smaller than in the subsequent bending in order to suppress the excessive curvature that otherwise would be produced in the first bending as shown in Fig. 5.

Figure 8 shows the displacements of the center roller which are required for various values of

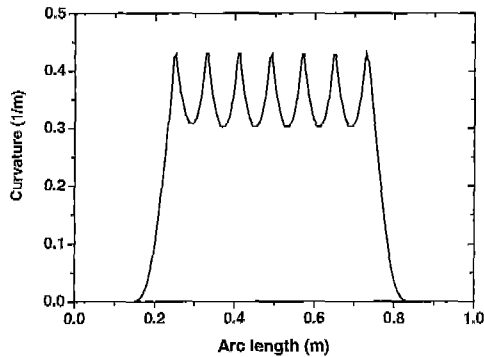


Fig. 7 Curvature distribution obtained by sequential bending prescribed by Fig.6

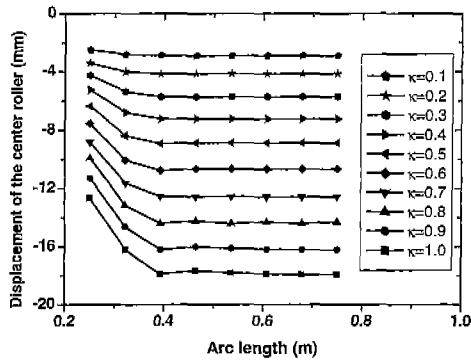


Fig. 8 Displacements of center roller for various constant curvatures

constant curvature. It may easily be seen from Fig. 8 that all curves are similar to those in Fig. 6 and that more displacement is required in order to achieve greater curvature.

#### 4. Finite Element Analyses

Finite element analyses were conducted in this work for two reasons. The primary reason was to analyze the real roll bending process as closely as possible, for example, by modeling the complex contacting mechanism described in Section 2. The secondary reason was to investigate the stress and strain components both during and after the process.

##### 4.1 Finite element models

The problem is first analyzed in one dimension by modeling the plate with the beam elements.

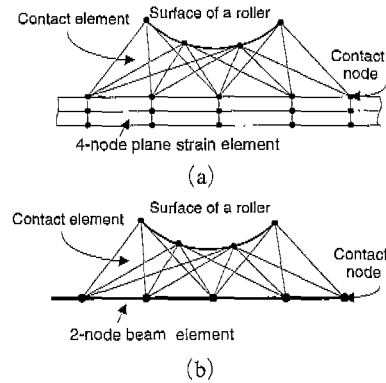


Fig. 9 Finite element models for contacting surfaces using (a) plane strain elements, and (b) beam elements, for the plate

This analysis was conducted to obtain a direct comparison with the analytical approach that is based on the beam theory. The problem is then analyzed in two dimensions by modeling the plate with plane strain elements. These two finite element models are schematically shown in Figs. 9 (a) and 9(b), respectively. In both cases, the rollers are all assumed to be rigid.

To properly model the contacting mechanism explained in Section 2, the so-called contact elements, which are widely used to analyze collision problems, are employed between the contacting bodies (see Fig. 9). The contact elements preclude the prohibited inter-penetration of the contacting bodies and model the mutually acting normal compressive forces. It is assumed that no slip occurs between the plate and rollers. Also, in order to guarantee a unique solution, the horizontal displacement at point *B*, shown in Fig. 1, is set to zero as a reasonable geometrical boundary condition. The feeding of the workpiece is simulated by slight horizontal translations of the three rollers.

The finite element analyses were performed using ANSYS, a commercial FEA package. All geometrical and material properties used are the same as listed in Table 1.

##### 4.2 Numerical results and comparisons

Figures 10 and 11 show the curvature distributions obtained by the FEA with the beam

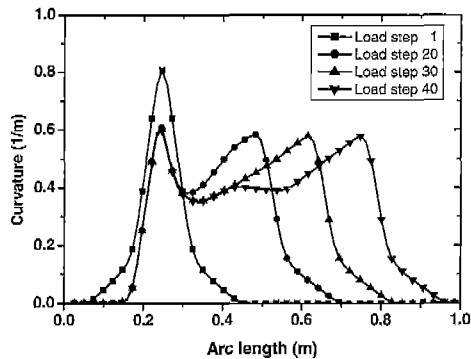


Fig. 10 Curvature distribution at various load steps, obtained by FEA with beam elements

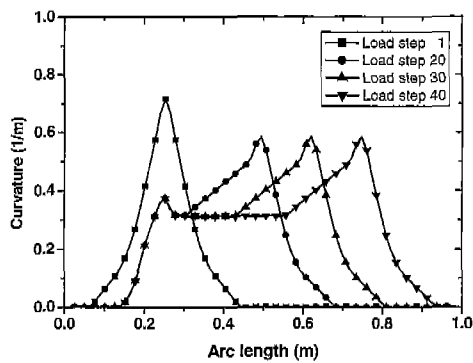


Fig. 11 Curvature distribution at various load steps, obtained by FEA with plane strain elements

elements and the plane strain elements, respectively. It is assumed that the rolling region of the plate, 0.5 m long (see Table 1), is bent by forty equally spaced sequential bending operations (hence,  $s_b = 500 \text{ mm}/40 = 12.5 \text{ mm}$ ) with the same constant displacement of the center roller,  $Y_c = 7.5 \text{ mm}$ , as in the analytical approach. Each curve in Figs. 10 and 11 represents the curvature distribution at the indicated bending sequence (or load step); that is, curvatures under loading, and not the residual curvatures after unloading, are shown. For this reason, all curves, except those for Load step 1, exhibit a big rear bump immediately before descending to zero. Each of these rear bumps is, of course, located at the location corresponding to the center roller. Residual curvatures after unloading are not shown here, but are approximated by removing or significantly reducing the rear bumps in Figs. 10 and 11.

Several observations may be made from these figures.

Firstly, since the entire bending process is modeled by a sufficient number of sequential bending operations, the curvature distributions are very smooth, in contrast to the result of the analytical approach, as shown in Fig. 5. Secondly, it should be noted that Fig. 5, without the fluctuations due to discretization, and the curve for Load step 40 in Fig. 10, without the rear bump, are in good qualitative and quantitative agreement. This agreement would have easily been expected from the fact that both results are based on the modeling of the plate as a beam. Further, this consistency between two results indicates that the effects of the complex contacting mechanism modeled only in the FEA are not great for smoothly curved plates such as being considered in this study. Finally, a comparison between Figs. 10 and 11 reveals that the "undershoot" effect is much less severe (or not observable) in the case of plane strain elements than in the case of beam elements. This is because the curvature produced by the first bending with plane strain elements is not sufficient to cause an "undershoot" in the subsequent bending. This smaller curvature in the case of plane strain elements is, in turn, due to the greater stiffness of plane strain elements compared to the beam elements.

Using FEA, stress and strain components have been investigated, and several features of the mechanics involved in the process have been observed (Kim, 1996). However, only one feature is discussed in this paper. Figure 12 shows the distributions of residual bending strains after unloading, throughout the cross section of a plate which is located directly below the center roller. The total bending strain is composed of elastic and plastic components. Both components are linearly distributed throughout the thickness. The small, but nonzero elastic strain component,  $\epsilon_x^e$ , shown in Fig. 12 indicates that nonzero residual stress exists.

The greatest practical interest lies in determining the relationship between the center roller displacement and the residual curvature. To

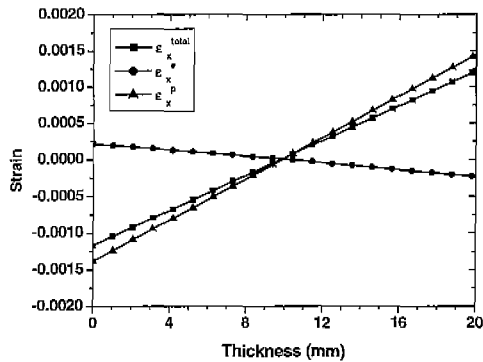


Fig. 12 Distribution of residual bending strains along the plate's thickness after unloading

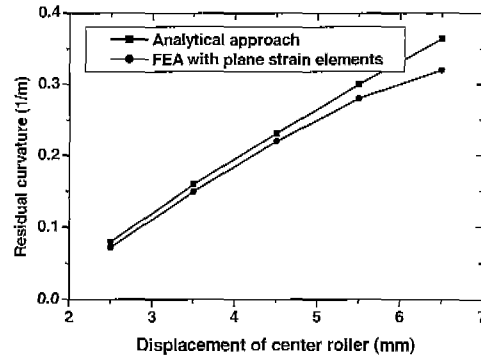


Fig. 13 Relationship between displacement of center roller and residual curvature

obtain this relationship by FEA, the inverse problem has been solved for several values of desired residual curvature. Figure 13 shows the constant residual curvatures versus the required steady-state displacements of center roller, obtained by FEA with plane strain elements and by the analytical approach. It may be stated here that, although the actual bending process is better modeled by the finite element method, the analytical approach based upon the simple three-point bending beam theory may still be used without introducing significant errors. The reason why the FEA predicts smaller curvature is due to the reduced degree of freedom in deformation, resulting from the fuller consideration of contact between the rollers and workpiece in FEA. Also, the deviation of analytical results in Fig. 13 from the FEA results is allowable in real shipyards because the analytical approach will certainly provide a much more logical and better methodology compared to the current experience-based practice, and because conducting FEA every time when needed is not practical at all.

It should be noted here that this analytical approach does not hold for the bending of a rectangular plate along an oblique direction or for bending non-rectangular plates, since the beam theory is no longer applicable. Various non-rectangular shapes of plates are indeed fabricated in the actual shipyards and, for those cases, the finite element analysis approach proposed in the paper will be required.

## 5. Conclusions

The mechanics of the three-roll bending process for smoothly curved plates has been studied by an analytical approach and by the finite element method. The primary objective of this study is to develop a logical and accurate procedure for determining the center roller displacement required for the fabrication of a plate with the desired curvature. The procedure in the analytical approach has been obtained by modifying and extending an existing model based on the beam theory. The finite element model with plane strain elements is much closer to the actual process: for example, the complex contacting mechanism between the rollers and the plate is accurately modeled by use of the contact elements.

The results of both analytical and finite element approaches have been investigated and compared with each other. In particular, the steady-state displacement of the center roller which is required for a constant curvature has been obtained by both approaches. As a result, the findings show that the simple analytical approach yields sufficiently accurate results for smoothly curved plates. Therefore, it may be concluded that the procedure in the analytical approach, based on the beam theory, may be used to determine the center roller displacement. A potential use of this procedure would be for the real-time computation that will be necessary for automation of the process.



This paper represents intermediate results of our work to logically determine all parameters of the roll bending process. In order for the analytical procedure proposed in this study to be useful in practice and actually applied, further development will be needed. For example, an analytical procedure that can handle non-rectangular plates and non-constant curvatures must be developed. Finally, the method proposed in this study will need to be verified against experimental results. Yet, this will require cooperation of shipyards, and development of new techniques to measure curvature distributions. Efforts are being made to this end.

### References

- Hansen, N. E. and Jannerup, O., 1979, "Modeling of Elastic-Plastic Bending of Beams Using a Roller Bending Machine," *Journal of Engineering for Industry*, Vol. 101, pp. 304~310.
- Hardt, D. E., Wright, A., and Constantine, E., 1990, "A Design-Oriented Model of Plate Forming for Shipbuilding," *Journal of Ship Production*, Vol. 6, No. 4, pp. 212~218.
- Hardt, D. E., Constantine, E., and Wright, A., 1992, "A Model of the Sequential Bending Process for Manufacturing Simulation," *Journal of Engineering for Industry*, Vol. 114, pp. 181~187.
- Kim, Y. I., 1996, *Analysis of Plate Bending by Pyramid Type Three-Roll Bending Machine*, Master's Thesis, Department of Naval Architecture and Ocean Engineering, Seoul National University.
- Oh, S. I. and Kobayashi, S., 1980, "Finite Element Analysis of Plane-strain Sheet Bending," *International Journal of Mechanical Science*, Vol. 22, pp. 583~594.
- Timoshenko, S. P., and Woinowsky-Krieger, S., 1959, *Theory of Plates and Shells*, McGraw-Hill, Inc.
- Shin, J. G., Park, T. J., and Yim, H., 2001, "Kinematics-Based Determination of the Rolling Region in Roll Bending for Smoothly Curved Plates," *Journal of Manufacturing Science and Engineering*, (accepted for publication).
- Yang, M. and Shima, S., 1988, "Simulation of Pyramid Type Three-roll Bending Process," *International Journal of Mechanical Science*, Vol. 30, No. 12, pp. 877~886.
- Yang, M., Shima, S., and Watanabe, T., 1990, "Model-based Control for Three-Roll Bending Process of Channel Bar," *Journal of Engineering for Industry*, Vol. 112, pp. 346~351.